Korean J. Chem. Eng., 36(10), 1648-1656 (2019)
DOI: 10.1007/s11814-019-0357-0

pISSN: 0256-1115
eISSN: 1975-7220

Modeling the performance of HPA membrane for sulfate ion removal from Ternary ion system

Shailendra Bajpai†, Robin Marlar Rajendran, and Sanjeevani Hooda

Department of Chemical Engineering, Dr B R Ambedkar National Institute of Technology, Jalandhar, 144011, India
(*Received 6 April 2019 • accepted 8 August 2019*)

Abstract−Sulfate removal from an aqueous system having ternary ions consisting of sodium and magnesium cations was modeled using Donnan-Steric-Pore model (DSPM). The ability of DSPM to characterize a membrane on the basis of diffusion, convection and electromigration (Donnan effect) makes it suitable for this process. A flat sheet hydrophilized polyamide (HPA50) nanofiltration membrane was used for experimental work. Membrane parameters such as hydraulic permeability ($4.2*10^{-12}$ m^3 m^{-2} s^{-1} Pa^{-1}), effective pore radius (r_p) and membrane charge density (X_m) were estimated. The effect of various operating parameters such as feed concentration, transmembrane pressure and feed flow rate was also studied for membrane performance. The model prediction was compared with the experimental data, and it was found that model prediction ability was excellent. The model was capable of predicting permeate concentration, and rejection percentage within 8% error was observed. This confirms the efficacy of our proposed model.

Keywords: Nanofiltration, DSPM, Ternary Ion System, Sulfate, HPA50

INTRODUCTION

Water is a basic necessity required for the survival. In many parts of India the availability of drinking water is very low. This scarcity is due to water pollution caused by urbanization (surface runoff of rainwater), industrialization (untreated discharge from industries) and human wastes flowing into the water bodies and also polluting groundwater resources. The main source of drinking water in India, i.e., the groundwater, has reached the category of "unsafe" in major parts of India and has been found to contain anions such as chloride, nitrate, sulfate, and carbonate above acceptable limits [1]. According to the Central Water Commission (CWC) and the Central Ground Water Board (CGWB) of India, if the demand for water and pollution of drinking water sources continues in the same pattern, then half of the water demand of India will be unmet by 2030 [2].

Sulfate concentration in drinking water is one of the important considerations among anions which has an acceptable limit of 200 mg/L as per Central Pollution Control Board (CPCB) of India [3]. Limitation of guidelines and regulations shows that sulfate discharge into water bodies was a concern. According to a groundwater quality report by CPCB, many drinking water resources in India are exceeding the acceptable limits of sulfates [4]. And sulfate is significant impurity in mining waters [5]. The origins of sulfate ions in ground water are sulfate ores, industrial waste, saline water intrusion, and atmospheric sulfur dioxide. Elevated sulfate levels (>500 g/L) can have a laxative effect on humans, noticeable taste in drinking water [6] and overall harmful effect on human health.

Many methods are being employed to treat the wastewater coming as effluents from industries and other sources before discarding it as well as to treat the groundwater before supplying it to households. One of these methods used, pressure driven membrane separation process (MSP), is important in the present context. The widely preferred MSPs are reverse osmosis [7], nanofiltration [8], ultrafiltration [9], and microfiltration [10]. These processes are used to remove varied sizes of components ranging from metal ions to suspended solids. Although out of all the membrane processes reverse osmosis (RO) is considered to be able to treat wastewater and drinking water fully by only allowing water to pass through it, but it has its disadvantages as it also removes the essential minerals required in the water [11]. Whereas NF process removes the contaminants from the water while maintaining the proper quality of the water by preserving the minerals essential for the human body. It is more of an efficient process in comparison with RO because of its ability to separate not only on the basis of size (steric effect) but also on the basis of electric charge (Donnan effect) of the ions being separated. This property of NF membrane makes it an important commodity in separation processes. NF membrane is used for treating groundwater, surface water as well as wastewater [12]. This process is also efficient and cost effective in comparison with other conventional processes like flocculation, coagulation, media filtration etc., for many industries like textile, pharmaceuticals and petroleum [13]. Moreover, negatively charged membranes are more suitable for anion removal such as sulfate.

As per Oatley-Radcliffe et al., applications of NF membrane are growing in various industries; the trend in NF research has increased in the last decade and many areas have been explored like membrane modification, membrane synthesis, modeling, desalination, and fouling studies. They concluded that the research done in the area of desalination is only 8.94% and in modeling 6.78% only [14]. In literature, modelling by using binary solute system has been extensively studied, whereas limited research has been done on multiple solute system.

†To whom correspondence should be addressed.
E-mail: bajpais@nitj.ac.in

Some researchers have worked with NF membranes to remove the divalent salts [15,16] whereas others to remove heavy metals like lead, arsenic, chromium, and cobalt ions from the water [17,18]. However, real groundwater consists of multiple solutes. It is therefore important to study a multiple solute system to make the research work closer to reality. Mohammad et al. [19] have worked with NF membrane to study the rejection of multicomponent salts mixture of NaCl and Na_2SO_4 at varying pore radius, membrane charge density and varying NaCl : Na_2SO_4 [19]. However, they have not studied the effect of concentration on the membrane charge density in the presence of divalent cations like Ca^{2+} or Mg^{2+}. Similarly, other researchers have worked with the ternary ion system [20], but very few have done the study in order to observe the variation in rejection % of the solute ions with respect to the various operating conditions such as transmembrane pressure, feed concentration and feed flow rate simultaneously.

Donnan-Steric-Pore Model (DSPM) considers the transport of ion on the basis of diffusion, convection and electromigration and is based on electroneutrality condition. It is derived from the extended Nernst-Planck equation and is successful in predicting the rejection of solutes [21]. This model uses three important membrane parameters--effective pore radius (r_p), the ratio of an effective membrane thickness to the porosity ($\Delta x/\varepsilon$), and an effective membrane charge density (X_M)--based on which it characterizes the membrane.

The transport mechanism of the NF process has been widely studied for a binary system. However, not much work has been done to understand the separation of multiple solute system. In this paper, sulfate ion removal from aqueous system having ternary ions consisting of sodium and magnesium cations was studied using flat sheet hydrophilized polyamide (HPA50) nanofiltration membrane. The efficacy of HPA50 membrane for sulfate removal from aqueous solution was studied for various operating parameters. The effect of feed concentration, transmembrane pressure (TMP), and feed flow rate on membrane performance was studied. Important membrane parameters, such as pore radius (r_p) and membrane charge density (X_m), were estimated and sulfate ion rejection in permeate stream was predicted using Donnan steric pore model. The model predictions were tested with experimental data.

THEORY

Transport of ions in membrane can be explained by the modified extended Nernst-Planck (ENP) equation, which covers hindrance transport inside pores in convective transport [21]. The membrane is assumed to be porous and contains cylindrical pores. The velocity inside the pore has parabolic profile of the Hagen-Poiseuille type, and it is homogeneous in the x direction. Potential gradient is assumed to be common for every ion inside the membrane. The below equation represents transport of ions due to diffusion, electric field gradient and convection respectively.

$$j_i = -D_{i,P}\frac{dc_i}{dx} - \frac{z_i F c_i D_{i,P}}{R_g T} * \frac{d\varphi}{dx} + K_{i,c} c_i V \quad (1)$$

where, hindered factor for convection is accounted by the term $K_{i,c}$ which is related to hydrodynamic lag co-efficient and steric hindrance factor [$K_{i,c}=(2-\Theta_i)(1+0.054\lambda_i-0.988\lambda_i^2+0.441\lambda_i^3)$]; The center line approximation range is $0<\lambda<0.8$ for the selected system; c_i is concentration of ion 'i' solute within pore, z_i=valence of ion; F is faraday constant, R_g is Gas constant, T is Temperature in K. Pore diffusivity $D_{i,p}=K_{i,d}D_B$; where, $K_{i,d}$ is hindrance factor for diffusion ($K_{i,d}=1-2.3\lambda_i+1.154\lambda_i^2+0.224\lambda_i^3$), D_B is bulk diffusivity.

From the continuity equation in the membrane and the permeate, the molar flux of component 'i' can be correlated to the permeate concentration ($C_{i,P}$) and the velocity (V) inside the membrane defined from a solute material balance:

$$J_i = C_{i,P} * V \quad (2)$$

where, $C_{i,P}$ is permeate concentration of an ion 'i', V is solvent velocity. From Eqs. (1) and (2), the concentration gradient of an ion 'i' in a solution can be derived,

$$\frac{dc_i}{dx} = \frac{V}{D_{i,P}}(K_{i,c} * c_i - C_{i,P}) - \frac{z_i F c_i}{R_g T} * \frac{d\varphi}{dx} \quad (3)$$

The equations of electroneutrality in the membrane and the bulk are used in this model as:

$$\Sigma z_i c_i + X_M = 0 \text{ (In membrane)} \quad (4)$$

$$\Sigma z_i C_i = 0 \text{ (in Bulk)} \quad (5)$$

where, c_i is concentration of ion 'i' solute within pore; C_i is bulk concentration; z_i is valence of ion 'i', and X_m is membrane charge density.

The potential gradient of an ion 'i' in a solution is obtained by differentiating Eq. (4),

$$\frac{d\varphi}{dx} = \frac{\Sigma_{1=1}^{n} \dfrac{z_i V (K_{i,c} * c_i - C_{i,P})}{D_{i,P}}}{\dfrac{F}{R_g T} * \Sigma_{i=1}^{n} z_i^2 c_i} \quad (6)$$

The solution of the above equation is performed iteratively applying the boundary conditions derived from Donnan steric partioning equation. The distribution of ion inside the membrane is expressed through Donnan effects:

$$\frac{c_i}{C_i} = \Theta_i * \exp\left(-\frac{z_i F}{R_g T}\Delta\varphi_D\right) \quad (7)$$

where, $\Delta\varphi_D$ is Donnan potential. The value of the Donnan potential is assumed to be the same for all ions at the membrane surface in the solution.

MATERIALS AND METHODS

1. Chemicals and Membrane Used

All chemicals used for the experimental work were analytical grade and procured from S.D. Fine Chemicals, India and Chong yu Hi-tech Chemicals, China. Desired quantity of sodium sulfate and magnesium sulfate was used to prepare feed solution. Chemicals like sodium chloride, hydrochloric acid, ethanol, glycerol and barium chloride were used to analyze the concentration of sulfate ion [22]. A hydrophilized polyamide (HPA50) nanofiltration membrane was used for experimental studies. The membrane was sup-

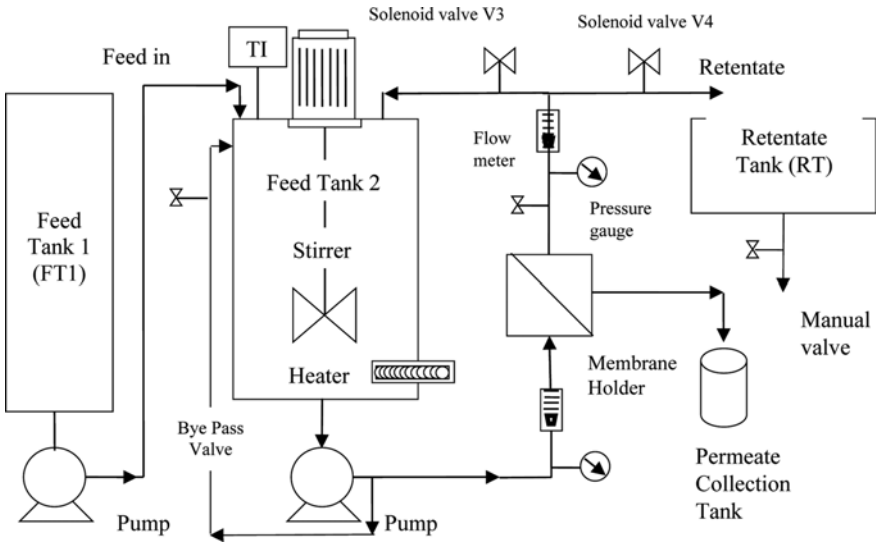

Fig. 1. Schematic diagram of the experimental setup (NF Test Cell).

plied by Permionics Membranes Pvt. Ltd., India. The surface area of the membrane was 100 cm^2 and HPA50 was used as a flat sheet membrane module.

2. Experimental Setup and Method Used

Experiments were conducted on an NF test cell, which is shown in Fig. 1. The feed solution was first kept in a stainless steel feed reserve tank (FT1) from where it was transferred to the feed tank (Feed Tank 2) that has the capacity for 5 L. The feed then was pumped through high pressure. The retentate can either be drawn in a retention tank (RT) or can be bypassed back through the valve (V3) to feed tank for a continuous system. Permeate was collected in the container at atmospheric pressure. The feed pressure was adjusted using valve V1 and by changing the speed of the motor. The feed flow rate was changed using the valve V2 and V3. The feed pressure and reject pressure were measured using pressure gauges PG1 and PG2. The feed flow and permeate flow were measured using rotameters FM1 and FM2.

Aqueous ternary feed solution of sodium, magnesium, and sulfate ion was prepared of three different concentrations by dissolving the desired quantity of Na_2SO_4 & $MgSO_4$ salts in deionized water. The individual salt concentration was in the ratio of 50 : 50 molar ratio. Experiments were conducted at three different feed flow rates (0.9, 1.2 and 1.8 m^3/s), feed concentrations (270, 405 and 540 mg/L) and feed pressures (2, 3 and 4 kg(f)/cm^2). For each run, before collecting the samples for analysis, the unit was operated for about 20 minutes to ensure steady state. UV-visible spectrophotometer (Shimadzu UV 2600 series, Japan make) was used to analyze the concentration of sulfate ion.

RESULTS AND DISCUSSION

1. Estimation of Membrane Parameters

1-1. Estimation of Hydraulic Permeability (L_p)

Hydraulic permeability (L_p) is calculated using deionized water as the feed in the test cell and at varying transmembrane pressure. Hydraulic Permeability is the standard characterization method to measure the maximum solvent permeability through the membrane. The equation used for hydraulic permeability estimation is:

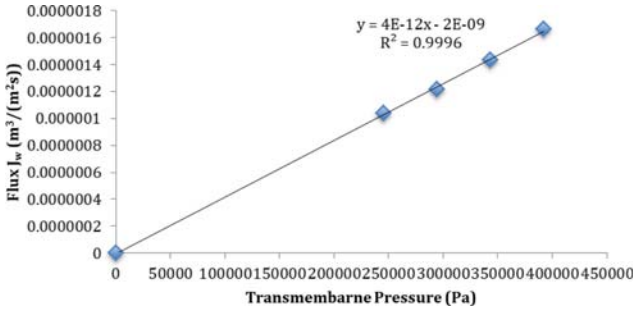

Fig. 2. Graph between transmembrane pressure and permeate flux to estimate hydraulic permeability.

$$J_w = L_p \cdot \Delta P \tag{8}$$

where, J_w is solvent permeability, ΔP is transmembrane pressure. The hydraulic permeability is estimated from Fig. 2 and it comes out to be $4.2*10^{-12}$ m^3 m^{-2} s^{-1} Pa^{-1} at 298 K. Similar values have been reported by literature for NF test cell module [23,24].

1-2. Estimation of Pore size (r_p)

Pore radius is one of the significant parameters in membrane characterization. The equations were selected for cylindrical pores with respect to center line approximations. The fundamental transport equation for uncharged solute rejection is;

$$R = 1 - \left(\frac{C_P}{C_F}\right) = 1 - \frac{\Theta}{1 - (1 - \Theta) \cdot \exp(-P_e)} \tag{9}$$

where, Θ_i is steric hindrance factor [$\Theta_i = (1-\lambda_i)^2$]; λ_i is friction factor, [$\lambda_i = \frac{r_i}{r_p}$]; r_i is solute radius; r_p is pore radius, and the P_e, Peclet number, can be written in terms of transmembrane pressure as shown in Eq. (10).

$$P_e=\frac{r_p^2\cdot\Delta P}{8\cdot\eta\cdot D_p} \tag{10}$$

where, ΔP is transmembrane pressure; $D_{i,p}$ is the pore diffusivity of ion 'i'[$D_{i,P}=K_{i,d}\cdot D_B\cdot\frac{\eta}{\eta_0}$]. Bulk diffusivity (D_B) is corrected using hindrance factor and viscosity relation; viscosity relation and pore diffusivity are given in literature [15]. Eq. (11) claims the average viscosity in terms of area

$$\frac{\eta}{\eta_0}=1+18\cdot\left(\frac{d}{r_p}\right)-9\cdot\left(\frac{d}{r_p}\right)^2 \tag{11}$$

Dynamic viscosity (η_0) of water is calculated from Slott Equation [25]

$$\eta_0=0.59849\cdot(43.252+T)^{-1.5423} \tag{12}$$

An iteration program was developed in MATLAB software to determine the effective pore size of the membrane. The working equations used in these iteration calculations are discussed above. Feed concentration, permeate concentration, and transmembrane pressure were given as input details in the developed iteration program. Pore size was iterated until the rejection values (calculated and measured) were affirmed for the given error range. Pore size evaluation is important for the economics of the system. The average pore radius was 0.321 nm, which was employed later to analyze the salt rejection. Estimated value is similar to other polyamide membranes [15,26].

Note that the Stokes radius of sulfate ion was taken as 0.23 nm from literature [27,28] for calculation. Pore radius of the nanofiltration membrane was estimated as 0.321 nm based on the equation used in the Donnan steric pore model and our experimental results. Pore size distribution is an important parameter, especially in microporous ultra-filtration (Michaelis equation) process where rejection of solute is mainly dependent on pore size distribution. However, in the nanofiltration process, diffusion, convection, steric hindrance, charge of solute, charge of NF membrane, solute concentration, solution pH are the dominant factors for rejection of solute.

1-3. Estimation of Membrane Charge Density (X_m)

Membrane charge density is the result of surface charge on the exterior membrane surface, and in the interior pore surface. Factors influencing the rejection of the salt in a solution are the interaction of the ions present in the solution and ions present on the surface of a charged membrane. The DSPM was applied to ternary mixture systems. Eq. (7) was applied for ions Mg^{2+} and SO_4^{2-} and also for ions SO_4^{2-} and Na^+ which gives the following equations:

$$\left(\frac{c_1(0)}{\Theta_1 C_{1,F}}\right)^{0.5}=\left(\frac{c_2(0)}{\Theta_2 C_{2,F}}\right)^{-0.5} \tag{13}$$

$$\left(\frac{c_2(0)}{\Theta_2 C_{2,F}}\right)^{-0.5}=\left(\frac{c_3(0)}{\Theta_3 C_{3,F}}\right) \tag{14}$$

As per the order of ion assumed for ternary ion system, the electroneutrality of membrane can be written as follows from Eq. (4):

$$2c_1-2c_2+c_3+X_M=0 \tag{15}$$

where, c_1, c_2, and c_3 are the concentrations of magnesium, sulfate, and sodium ion, respectively, within membrane pores. Substituting Eq. (13) in (14) gives the quadratic equation which can be solved to obtain the boundary condition of sulfate ion at feed side and permeate side:

$$c_2(0)=\frac{0.5(c_3+x_M)+\sqrt{0.25(c_3+x_M)^2+4\Theta_1\Theta_2 C_{1,F}C_{2,F}}}{2} \tag{16}$$

$$c_2(\Delta x)=\frac{0.5(c_3+x_M)+\sqrt{0.25(c_3+x_M)^2+\left(4\Theta_1\Theta_2\left(C_{S,P}-0.5\cdot\left(\frac{c_2\cdot c_3^2}{\theta_3^2\cdot\theta_2\cdot C_P}\right)^{0.5}\right)\cdot C_{S,P}\right)}}{2} \tag{17}$$

where, $c_2(0)$ is boundary condition of concentration at feed side (x=0), $c_2(\Delta x)$ is boundary condition concentration at permeate side (x=Δx), $c_{2,avg}$ is average sulfate ion concentration in membrane [$c_{2,avg}=\frac{c_2(0)+c_2(\Delta x)}{2}$]; and Δc_s is sulfate ion concentration difference in membrane [$\Delta c_2=c_2(\Delta x)-c_2(0)$]. Concentration of sulfate ion in permeate can be expressed as:

$$C_{S,P}=\frac{-(4\cdot c_{2,avg}-c_3-2\cdot x_M)\cdot\Delta c_2}{4\cdot(P_{e1}+P_{e2})\cdot c_{2\,avg}-P_{e2}\cdot(2\cdot x_M+c_2)} \tag{18}$$

$$4\cdot(P_{e1}+P_{e2})c_{2\,avg}^2+c_{2\,avg}\left[(-2\cdot P_{e1}-P_{e2}+2\cdot P_{e3})-2\cdot x_M\cdot(P_{e1}+P_{e2})+2\cdot(P_{e1}-P_{e3})\cdot\sqrt{\left(\frac{c_2\cdot c_3^2}{\theta_3^2\cdot\theta_2\cdot C_{S,P}}\right)}\right]$$

Membrane charge density for HPA50 membrane was predicted using a software program developed in MATLAB. Donnan potential value at membrane interface is the same for all the ions in the solution [29]. This can be expressed through both the Donnan and steric effects (Donnan-steric partioning) as mentioned in Eq. (7). Applying this equation for components 1 (Mg^{2+} ion) and 2 (SO_4^{2-} ion) gives Eq. (13). The same can be applied for components 2 (SO_4^{2-} ion) and 3 (Na^+ ion) that gives Eq. (14). Electroneutrality condition was applied to Eq. (13), which gives boundary conditions at pore inlet ($c_2(0)$) and pore outlet ($c_2(\Delta x)$); $c_2(0)$ is the function of feed concentration of Mg^{2+} ion and SO_4^{2-} ion [$C_{1,F}$ and $C_{2,F}$]. At the same time, $c_2(\Delta x)$ is the function of permeate concentration of Mg^{2+} ion and SO_4^{2-} ion [$C_{1,P}$ and $C_{S,P}$]. X_m value was assumed to calculate pore inlet concentration ($c_2(0)$), and pore outlet concentration ($c_2(\Delta x)$), using Eqs. (16) and (17). Permeate concentration value was iterated between 0 to feed concentration and the developed program iterated by Bi-section method for the assumed X_m value. Iteration continued until Eq. (18) was satisfied with the iterated value. The membrane charges estimated earlier were used to calculate the permeate concentrations from the linearized model. Finally, sulfate permeate concentration ($C_{S,P}$) was calculated using Eq. (18).

Variation of X_m was evaluated for the HPA50 membrane plotted against transmembrane pressure, as shown in Fig. 3. Concentration of salts plays an important role in membrane charge density

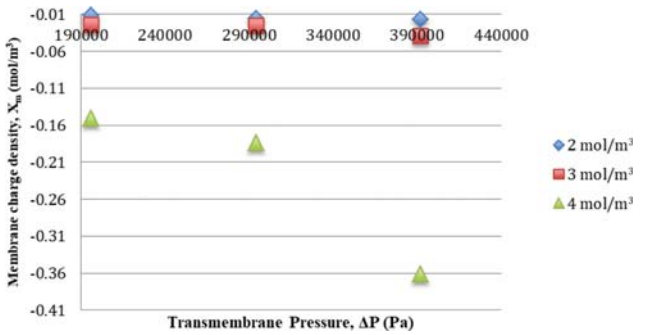

Fig. 3. Graph to show the variation of membrane charge density with respect to transmembrane pressure at constant feed flow rate.

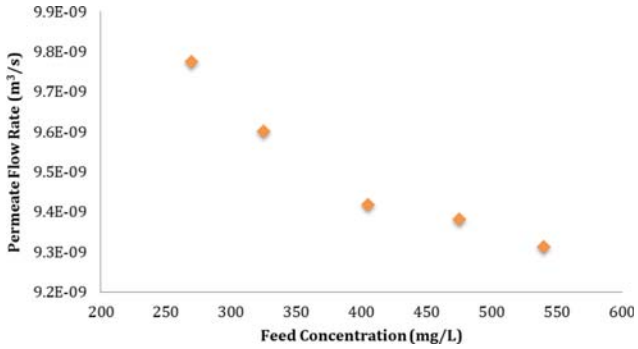

Fig. 5. Graph to show the variation of permeate flow rate with respect to feed concentration at constant pressure 196 kPa and feed flow rate 3.33*10^{-4} m^3 s^{-1}.

[30]. It is showing negative membrane charge density for all feed concentrations used in the present study, which plays a major role in exclusion of the SO_4^{2-} ions from the permeate stream. Generally, NF membranes possess positive or negative charge, which depends upon chemistry of feed solution and functional group of membrane [27]. HPA50 is a polyamide membrane that contains a functional group of carboxylic acid (-COOH). Dissociation of membrane functional group can be linked to fixed negative charge of the membrane in polymer matrix. And also, when an aqueous solution contacts a membrane surface, adsorption of anions (SO_4^{2-}) takes place. However, counter ions of the solutions get neutralized with the fixed surface charge of the membrane at lower feed concentrations. While increasing the feed concentrations, sulfate ions accumulation on membrane can lead to higher membrane charge density compared to lower feed concentrations (2 and 3 mol/m^3) as shown in Fig. 3. It affirms that X_m is not a constant value and can be correlated to feed concentration.

2. Effect of Parameters on Membrane Performance

2-1. Effect of Varying Feed Concentration

The variation in feed concentration at constant pressure and feed flow rate results in rejection percentage be seen from Fig. 4. There is a slight increase in rejection percentage of the solute while increasing feed concentration. There are chances of increase in solute concentration on the surface of the membrane, which increases the steric hindrance as well as possibly leading to back diffusion of the solute. This leads to increase in the rejection percentage of the solute. It can also be explained in a way by increasing feed concentration there will be an increase in the presence of divalent ions (SO_4^{2-}) in the feed solution which will not be able to pass through the pores of the membrane due to steric hindrance effect, which results in the increase in rejection percentage. Similar results are shown in the literature where the increase in feed concentration increases negative charge density on the membrane as shown in Fig. 3. Due to preferential sorption which in turn rejects the co-ion charge from passing through the membrane and to maintain electroneutrality [31].

The graph shown in Fig. 5 was plotted between feed concentration and permeate flowrate. It depicts the decrease in permeate flow rate by increasing the feed concentration keeping all other parameters constant. Osmotic driving force would increase while increasing feed concentration causes decrease in permeate flow rate as solute concentration on the membrane surface increases [32]. Similar results were found in the literature that with increase in feed concentration the volumetric flux decreases due to increase in osmotic pressure [31,33]. Hence if volumetric flux is decreasing then permeate flow rate also decreases.

2-2. Effect of Varying Transmembrane Pressure

Fig. 6 shows the variation in rejection percentage with changing transmembrane pressure at different concentrations. The feed flowrate was maintained at 3.33*10^{-4} m^3 s^{-1} while varying transmembrane pressure. There was a slight decrease in rejection percentage with increasing transmembrane pressure, which means an increase

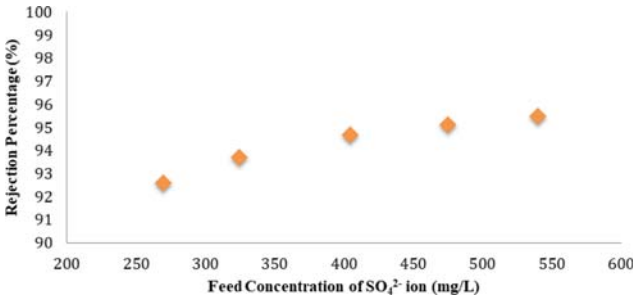

Fig. 4. Graph to show the variation of rejection percentage with respect to feed concentration at constant pressure 196 kPa and feed flow rate 3.33*10^{-4} m^3 s^{-1}.

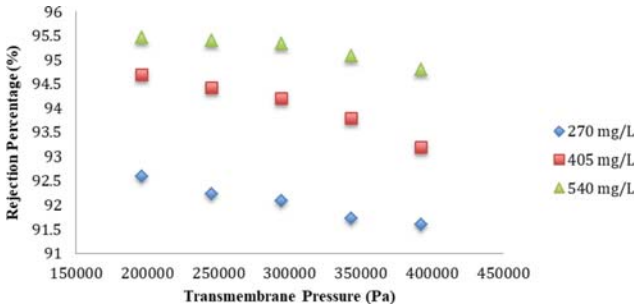

Fig. 6. Graph to show the variation of rejection percentage with respect to transmembrane pressure at constant feed flow rate 3.33*10^{-4} m^3 s^{-1}.

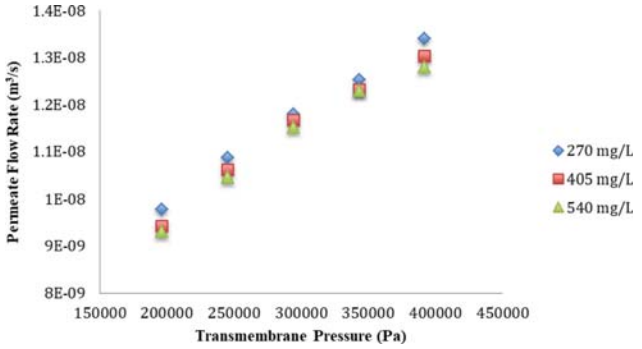

Fig. 7. Graph to show the variation of permeate flow rate with respect transmembrane at constant feed flow rate 3.33*10^{-4} m^3 s^{-1}.

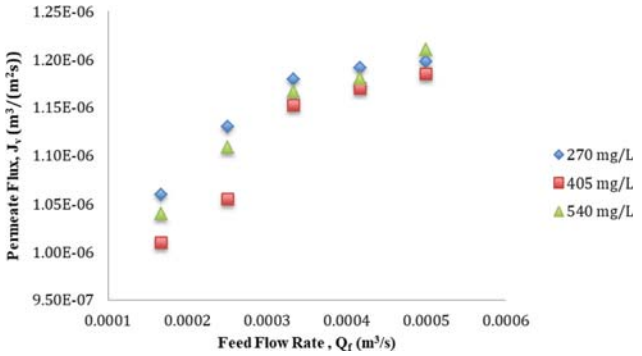

Fig. 9. Graph to show the variation of permeate flux with respect to feed flow rate at constant transmembrane pressure 196 kPa.

in the concentration of solute on permeate side. This can be explained on the basis of electroneutrality condition that allows the SO_4^{2-} ions to permeate through the membrane at high pressure leading to lower rejection. It can also be seen that the rejection percentage is high at lower concentration, which is mostly due to electrostatic exclusion and high ion size as depicted in Fig. 6. Permeate flow rate increases by increasing transmembrane pressure as shown in Fig. 7 because of driving force of mass transfer. It can also be viewed as discussed by Paugam et al., when the transmembrane pressure increases the driving force becomes higher than the surface force, which results increase in solvent flux [34]. At the same time, Q_p is almost similar for all the concentrations selected. It implies transmembrane pressure dominates over osmotic pressure in permeate flow.

2-3. Effect of Varying Feed Flow Rate

Fig. 8 shows the sulfate ion rejection percentage for various feed flowrates. As we increased the volumetric flow rate of the feed, the concentration of permeate was decreasing, which in turn was slightly increasing the rejection percentage of the solute. The rejection percentage variation for the studied flowrate was very less for all the concentration selected. It shows that feed flow rate has little or no

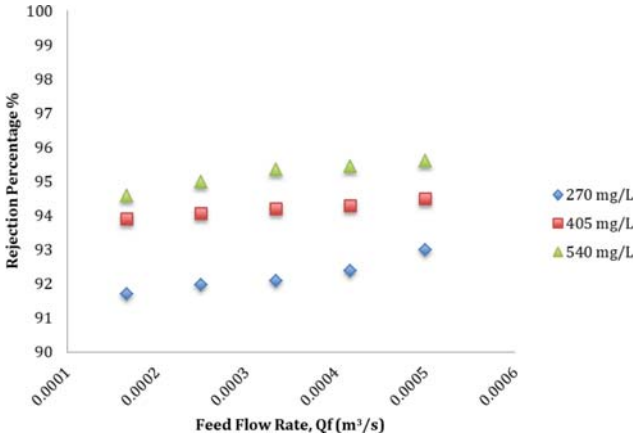

Fig. 8. Graph to show the variation of rejection percentage with respect to feed flow rate at constant transmembrane pressure 196 kPa.

effect on rejection percentage for studied flow regime. The graph shown in Fig. 9 predicts the increase in permeate flux by varying overall feed flow rate. The increase in feed flowing through the membrane in a cross flow regime helps for spontaneous reduction of concentration polarization due to increase in velocity. Reduction of concentration on membrane surface can lead to higher permeate flow. It can also be explained that the drag force becomes larger than the surface force, which leads to the removal of concentrated salt on membrane surface and hence increases the permeate flow rate in turn.

3. Prediction of Membrane Performance and Comparison with Experimental Data

It is evident that the transport mechanism of an NF membrane is governed by convection, diffusion and electromigration. The flow of co-ions present in the feed solution is mostly governed by diffusive force, whereas the electromigration force mostly governs the flow of counter-ions. In this work, the transport of sulfate ions through the membrane is restricted due to the presence of the negative charge on the surface of the membrane. The co-ions diffuse with the membrane surface and maintain the electroneutrality condition. The presence of Na^+ ions is expected to be more on the permeate side in comparison to other ions present in the feed due to its smaller size as well as its ability to diffuse through the membrane. Moreover, electroneutrality condition is maintained in the presence of Mg^{2+} ions, which are less likely to pass through the membrane in comparison to Na^+ ions due to their divalent charge and larger size.

In the present work, we have taken equimolar concentration of Na_2SO_4 and $MgSO_4$ as explained in section 2.2. We can increase concentration of monovalent/divalent cation by changing the molar ratio of salts. In case monovalent cations (Na^+) are increased with respect to divalent cation, Na^+ ions are likely to permeate through membrane leading to decrease in rejection of sulfate in order to maintain electroneutrality condition and Donnan-steric effect. It can also be due to shielding effect of cation on membrane surface, which leads to decrease in rejection. However, if divalent cations (Mg^{2+}) are more compared to monovalent cation, sulfate rejection is expected to be higher due to larger size, divalent charge, and strong hydration [34].

Donnan steric pore model was solved in MATLAB as explained in sections 3.1.2 and 3.1.3 to evaluate the simulated results of the

Table 1. Experimental and theoretical data on removal of sulfate ion in NF system

S. No.	Feed flow rate	Feed concentration	Transmembrane pressure	Sulfate permeate concentration		Error	Rejection (R)		Error
	Q_f (*10^{-4})	C_f	ΔP	(Expt)	(Theo)		(Expt)	(Theo)	
	m^3/s	mg/L	Pa	mg/L	mg/L	%	%	%	%
1.	3.33	270	196133	14.23	14.06	1.19	92.58	92.67	−0.09
2.	3.33	405	196133	15.31	15.27	0.26	94.68	94.69	−0.01
3.	3.33	540	196133	17.43	17.53	−0.57	95.46	95.43	0.02
4.	3.33	270	196133	14.23	14.66	−3.02	92.58	92.36	0.24
5.	3.33	270	294200	15.19	15.23	−0.26	92.08	92.06	0.02
6.	3.33	270	392266	16.14	16.12	0.12	91.59	91.60	−0.01
7.	3.33	405	196133	15.31	16.42	−7.25	94.68	94.29	0.40
8.	3.33	405	294200	16.73	16.57	0.95	94.19	94.24	−0.06
9.	3.33	405	392266	19.62	19.32	1.52	93.18	93.29	−0.11
10.	3.33	540	196133	17.43	17.52	−0.51	95.46	95.43	0.02
11.	3.33	540	294200	17.87	17.68	1.06	95.34	95.39	−0.05
12.	3.33	540	392266	19.94	19.55	1.95	94.80	94.90	−0.10
13.	2.5	270	294200	15.42	15.47	−0.32	91.96	91.94	0.02
14.	3.33	270	294200	15.19	15.27	−0.53	92.08	92.04	0.04
15.	5.0	270	294200	13.46	13.33	0.96	92.98	93.05	−0.07
16.	2.5	405	294200	17.09	16.98	0.64	94.06	94.10	−0.04
17.	3.33	405	294200	16.73	16.58	−0.89	94.19	94.13	0.05
18.	5.0	405	294200	15.87	15.75	−0.25	94.48	94.47	0.01
19.	2.5	540	294200	19.25	19.31	−0.31	94.98	94.97	0.01
20.	3.33	540	294200	17.87	17.75	0.67	95.34	95.37	−0.03
21.	5.0	540	294200	16.84	16.81	0.17	95.61	95.62	−0.01

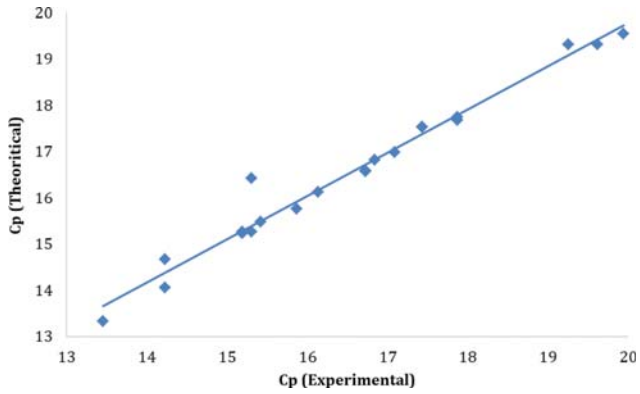

Fig. 10. Graph to show the consistency of permeate concentration obtained from experiments with the permeate concentration obtained theoretically.

membrane performance. The results of comparative study between the data obtained from linearized program and experimental data are shown in Table 1. From the data, the results obtained from the simulation work are in good agreement with experimental data. Graph shown in Fig. 10 depicts the consistency of the results obtained experimentally and theoretically. This confirms the excellent agreement of the model for ternary ion system. It was found that the percentage error calculated cameout to be less than 8% for permeate concentration and rejection percentage.

CONCLUSION

The efficacy of HPA50 membrane was studied for removal of sulfate ion from ternary ion system. The important membrane parameters were estimated. The hydraulic permeability of HPA50 membrane was found to be $4.2*10^{-12}$ m^3 m^{-2} s^{-1} Pa^{-1} which is commensurate with the literature values for similar module. The average pore radius was estimated as 0.321 nm. The membrane charge density (X_m) was calculated using bisection method, which was further used for estimating C_p value during simulation. It was found that the prediction of X_m value is not constant; it differs with feed concentration and in line with the reported literature. The effect of various operating parameters on membrane performance was also discussed. It has been found that Q_p and C_p values are increasing with transmembrane pressure and decreasing with feed concentration. Finally, the experimental data sets were used to simulate C_p and % R for ternary ion system using DSPM. The variation for C_p value was less than 8%. This shows the efficiency of proposed model in predicting the membrane performance.

ACKNOWLEDGEMENTS

The authors are thankful to the Ministry of Human Resource and Department (MHRD), Government of India for providing research grant to Ms. Sanjeevani Hooda and Mr. R. Robin Marlar.

NOMENCLATURE

A_m : membrane area [cm^2]
$c_i(0)$: concentration of ion 'i' within pore entrance [mg L^{-1}]
$c_i(\Delta x)$: concentration of ion 'i' within pore outlet [mg L^{-1}]
$c_{i,avg}$: average concentration of ion 'i' within pore [mg L^{-1}]
Δc_i : concentration difference of ion 'i' across the pore thickness [mg L^{-1}]
$C_{i,F}$, C_F : feed concentration of ion 'i' [mg L^{-1}]
c_i : concentration of ion 'i' within pore [mg L^{-1}]
$C_{i,p}$, C_p : concentrations in permeate of ion 'i' [mg L^{-1}]
$C_{S,P}$: sulfate ion concentrations in permeate [mg L^{-1}]
d : thickness of the oriented solvent layer [m]
D : diameter of the membrane [nm]
$D_{i,P}$: pore diffusivity of ion 'i' [m^2 s^{-1}]
D_B : bulk diffusivity [m^2 s^{-1}]
F : Faraday Constant [96487 C mol^{-1}]
i : concentration gradient of an ion 'i' in a solution
J_v : volumetric flux [m^3 m^{-2} s^{-1}]
$K_{i,d}$: hindered diffusion, dimensionless
$K_{i,c}$: convective diffusion, dimensionless
L : length of the membrane [cm]
L_p : hydraulic permeability [m^3 m^{-2} s^{-1} Pa^{-1}]
Pe : Peclet number, dimensionless
Q_f : feed flowrate [m^3 s^{-1}]
Q_p : permeate flowrate [m^3 s^{-1}]
$R_{calculated}$: calculated rejection, dimensionless
$R_{experimental}$: experimental rejection, dimensionless
R_g : gas constant [8.314 m^3 kPa mol^{-1} K^{-1}]
r_i : ionic radius [nm]
r_p : pore radius [nm]
T : temperature [K]
V : velocity of permeate [m s^{-1}]
X_m : membrane charge density [mol m^{-3}]
z_i : valence of an ion, dimensionless

Greek Symbols

φ_D : potential [V]
$\Delta\varphi_D$: donnan potential [V]
Θ : steric partition coefficient
Δc_1 : concentration difference in pore
Δx : membrane active layer thickness [μm]
ΔP : pressure difference [Pa]
η : viscosity in the pore [Pa s]
μ : chemical potential [J mol^{-1}]
γ : activity coefficient

Abbreviations

DSPM : donnan-steric-pore model
ENP : extended nernst-planck model (ENP Model)
FM : flow meter/rotameters
FT : feed tank
HDM : hydrodynamic model
LPM : litre per minute
MF : microfiltration
MSP : membrane separation processes
MWCO : molecular weight cut-off
NF : nanofiltration
P : pump
PG : pressure gauge
PT : permeate tank
RO : reverse osmosis
RT : retentate tank
SDIM : solution diffusion imperfection model
SDM : solution diffusion model
SK : spiegler kedem model
TFC : thin film composite
TMP : transmembrane pressure
UF : ultrafiltration
V : valve

REFERENCES

1. G. Venkatesan and G. Swaminathan, *J. Environ. Eng. Landsc. Manag.*, **17**, 1 (2009).
2. WaterAid India. Available at: http://wateraidindia.in/faq/drinking-water-problems-india. Accessed July 24 (2018).
3. M. Bhavan, B. Shah and Z. Marg, B U R E A U O F I N D I A N S T A N D A R D S (2012).
4. Central Pollution Control Board | Ministry of Environment, Forest and Climate Change, Government of India. 2018. Available at: http://cpcb.nic.in/publication-details.php?pid=MTM=. Accessed February 27 (2019).
5. P. Kinnunen, H. Kyllönen, T. Kaartinen, J. Mäkinen, J. Heikkinen and V. Miettinen, *Water Sci. Technol.*, **2017**(1), 194 (2018).
6. W. H. Organization, Guidel. Drink. Water Qual. (2004).
7. Z. V. P. Murthy and S. K. Gupta, *J. Memb. Sci.*, **154**(1), 89 (1999).
8. T. Balanyà, J. Labanda, J. Llorens and J. Sabaté, *Sep. Sci. Technol.*, **54**(1), 143 (2019).
9. X. Zhang, Z. Xu, L. Wang, X. Wang, Y. Zeng and G. Zhang, Recent Patents Eng. (2018).
10. A. I. Jokić, L. L. Šereš, N. R. Milović, Z. I. Šereš, N. R. Maravić, Ž. Šaranović and L. P. Dokić, *Membr. Water Treat.* (2018).
11. S.-H. Yoon, Classification of membranes according to pore size (2016).
12. A. Santafé-Moros, J. M. Gozálvez-Zafrilla and J. Lora-García, *Sep. Purif. Technol.*, **187**, 233 (2017).
13. C. Jiang, Y. Wang and T. Xu, Membrane Technologies for Biorefining, 135 (2016).
14. D. L. Oatley-Radcliffe, M. Walters, T. J. Ainscough, P. M. Williams, A. W. Mohammad and N. Hilal, *J. Water Process Eng.*, 164 (2017).
15. W. R. Bowen and J. S. Welfoot, *Chem. Eng. Sci.*, **57**(7), 1121 (2002).
16. J. Schaep, C. Vandecasteele, A. Wahab Mohammad and W. R. Bowen, *Sep. Purif. Technol.*, **22-23**, 169 (2001).
17. S. Ghorai and K. K. Pant, *Sep. Purif. Technol.*, **42**(3), 265 (2005).
18. C. V. Gherasim, K. Hancková, J. Palarčík and P. Mikulášek, *J. Memb. Sci.*, **490**, 46 (2015).
19. A. W. Mohammad and M. S. Takriff, *Desalination*, **157**(1-3), 105 (2003).
20. S. Déon, A. Escoda and P. Fievet, *Chem. Eng. Sci.*, **66**(12), 2823 (2011).
21. W. R. Bowen, A. W. Mohammad and N. Hilal, *J. Memb. Sci.*, **126**(1),

91 (1997).
22. B. of Indian Standards, IS 3025 (Part 24): Method of Sampling and Test (Physical and Chemical) for Water and Wastewater, Part 24: Sulphates (First Revision), n.d.
23. J. Lv, K. Y. Wang and T. S. Chung, *J. Memb. Sci.*, **310**(1-2), 557 (2008).
24. F. Fang Chang, W. Jun Liu and X. Mao Wang, *Desalination*, **334**(1), 10 (2014).
25. K. Bai and J. Katz, *Exp. Fluids*, **55**, 1704 (2014).
26. J. Straatsma, G. Bargeman, H. C. van der Horst and J. A. Wesselingh, *J. Memb. Sci.*, **198**(2), 273 (2002).
27. O. Labban, C. Liu, T. H. Chong and J. H. Lienhard V, *J. Memb. Sci.*, **521**, 18 (2017).
28. A. A. Hussain, M. E. E. Abashar and I. S. Al-Mutaz, J. King Saud Univ. - Eng. Sci. (2018).
29. W. R. Bowen, J. S. Welfoot and P. M. Williams, *AIChE J.*, **48**(4), 760 (2002).
30. C. Labbez, P. Fievet, A. Szymczyk, A. Vidonne, A. Foissy and J. Pagetti, *Sep. Purif. Technol.*, **30**(1), 47 (2003).
31. A. L. Ahmad and B. S. Ooi, *Chem. Eng. J.*, **156**(2), 257 (2010).
32. Z. V. P. Murthy and S. K. Gupta, *Desalination*, **109**(1), 39 (1997).
33. S. Senthilmurugan, A. Ahluwalia and S. K. Gupta, *Desalination*, **173**(3), 269 (2005).
34. L. Paugam, S. Taha, G. Dorange, P. Jaouen and F. Quéméneur, *J. Memb. Sci.*, **231**(1-2), 37 (2004).